

Experimental evidence and modeling studies support a synchronizing role for electrical coupling in the cat thalamic reticular neurons *in vivo*

Pablo Fuentealba,¹ Sylvain Crochet,¹ Igor Timofeev,¹ Maxim Bazhenov,² Terrence J. Sejnowski^{2,3} and Mircea Steriade¹

¹Laboratory of Neurophysiology, Faculty of Medicine, Laval University, Quebec City, Canada G1K 7P4

²The Salk Institute, Computational Neurobiology Laboratory, 10010 North Torrey Pines Road, La Jolla, CA 92037, USA

³Department of Biology, University of California, San Diego, La Jolla, CA 92093, USA

Keywords: halothane, intracellular recordings and staining, spikelets, spindling

Abstract

Thalamic reticular (RE) neurons are crucially implicated in brain rhythms. Here, we report that RE neurons of adult cats, recorded and stained intracellularly *in vivo*, displayed spontaneously occurring spikelets, which are characteristic of central neurons that are coupled electrotonically via gap junctions. Spikelets occurred spontaneously during spindles, an oscillation in which RE neurons play a leading role, as well as during interspindle lulls. They were significantly different from excitatory postsynaptic potentials and also distinct from fast prepotentials that are presumably dendritic spikes generated synaptically. Spikelets were strongly reduced by halothane, a blocker of gap junctions. Multi-site extracellular recordings performed before, during and after administration of halothane demonstrated a role for electrical coupling in the synchronization of spindling activity within the RE nucleus. Finally, computational models of RE neurons predicted that gap junctions between these neurons could mediate the spread of low-frequency activity at great distances. These experimental and modeling data suggest that electrotonic coupling within the RE nucleus plays an important role in the generation and synchronization of low-frequency (spindling) activities in the thalamus.

Introduction

The γ -aminobutyric acid (GABA)ergic neurons of the thalamic reticular (RE) nucleus provide inhibitory input to thalamocortical neurons and are crucially involved in the generation of spindles (Steriade *et al.*, 1985, 1987), an oscillation that characterizes early stages of natural slow-wave sleep and barbiturate anesthesia. It was recently shown in slices maintained *in vitro* that RE neurons of rats and mice are electrically coupled and that electrical synapses require Cx36 (Landisman *et al.*, 2002), the predominant type of connexins, proteins that comprise gap junction channels (Condorelli *et al.*, 2000; Rash *et al.*, 2000; Venance *et al.*, 2000). Parallel experiments also revealed dye-coupling in cat dorsal lateral geniculate (dLG) neurons *in vitro*, accompanied by spikelets that survived application of antagonists of fast chemical synaptic transmission and were reversibly blocked by the gap junction blocker carbenoxolone (Hughes *et al.*, 2002). Spikelets are considered to be the electrophysiological correlate of electrotonic coupling via gap junctions (Perez-Velazquez & Carlen, 2000).

In addition to interactions through conventional chemical synapses, thalamic neurons use electrical synapses that might promote the synchronization of normal brain rhythms as well as in paroxysmal activities. The RE nucleus has a pivotal role in both these oscillatory types. The synaptic interactions between RE neurons as well as their reciprocal relations with thalamocortical neurons are regarded as the

key elements in generating sleep spindles (Steriade *et al.*, 1993) and imposing inhibitory postsynaptic potentials on thalamocortical neurons during spike-wave seizures (Steriade & Contreras, 1995; Timofeev *et al.*, 1998; Avanzini *et al.*, 1999). In view of the above-mentioned results from *in vitro* experiments on juvenile animals demonstrating electrical synapses among rat RE neurons, we examined this topic *in vivo*, using intracellular recordings and staining of these inhibitory neurons in the adult cat, as well as computational models. Data showed the presence of spikelets during and outside RE cells' oscillatory activity, which were significantly different from excitatory postsynaptic potentials (EPSPs) and fast prepotentials (FPPs). These results have been published in abstract form (Fuentealba *et al.*, 2002).

Materials and methods

Animal preparation

Experiments were performed on adult cats (2.5–3.5 kg), deeply anesthetized with pentobarbital (25 mg/kg, i.p.), urethane (1.8 g/kg, i.p.) or ketamine-xylazine (10–15 mg/kg and 2–3 mg/kg, respectively, i.m.). All experiments were conducted in agreement with the guidelines of NIH and the committee for animal care at Laval University. When the cats showed the signs of deep anesthesia, the animals were paralysed with gallamine triethiodide and artificially ventilated with control of the end-tidal CO₂ concentration at \approx 3.5%. Body temperature was maintained at 36–38 °C. The depth of

Correspondence: M. Steriade, as above.

E-mail: mircea.steriade@pfs.ulaval.ca

Received 20 November 2003, revised 21 April 2004, accepted 26 April 2004

anesthesia was monitored continuously by EEG, and additional doses of anesthetics were administered at the slightest tendency toward low-voltage and fast EEG rhythms. At the end of experiments, animals were given a lethal dose of pentobarbital (50 mg/kg).

Electrophysiological recordings

Current-clamp recordings from thalamic RE neurons were performed using glass micropipettes (DC resistance, 30–60 M Ω). To avoid breaking of recording micropipettes, the cortex and white matter overlying the head of the caudate nucleus were removed by suction. The pipettes entered \approx 3 mm through the caudate nucleus to reach the rostral pole or the rostromedial sector of the thalamic RE nucleus. Pipettes were generally filled with 3 M solution of K-acetate and, in some experiments, with KCl or KAc containing 50 mM of QX-314. The stability of intracellular recordings was ensured by cysternal drainage, bilateral pneumothorax, hip suspension and by filling the hole over the thalamus with 4% agar solution. A high-impedance amplifier with active bridge circuitry was used to record and inject current inside the cells. Most intracellular recordings included in the database lasted for periods longer than 30 min. Simultaneous extracellular recordings were performed using up to four tungsten electrodes (10–15 M Ω ; Frederick Haer, Bowdoinham, WA, USA) inserted through the caudate nucleus, with an interelectrode distance of \approx 0.5 mm. Thalamic RE neurons were recognized by their long burst (> 50 ms) and the accelerando-decelerando bursting firing pattern (see Fig. 7A). For data acquisition system, we used Nicolet Vision (Middleton, WI, USA).

Data analysis and computational modeling

The extraction of spikelets and EPSPs was performed automatically using Mini Analysis Program (Synaptosoft Inc., GA, USA). The peaks of events were selected within 3-ms windows, considering only deflections with higher amplitude than 0.6 mV and half duration less than 10 ms. Rising phase was fitted with a single exponential between 10 and 90% of the peak, while decaying phase was fitted with a single exponential between 90 and 10% of the peak.

Three network models were simulated: (1) a circuit with two coupled RE neurons; (2) a one-dimensional chain of 100 RE cells; and (3) a two-dimensional network of 128 \times 128 RE neurons. In the one-dimensional network the diameter of the connection fan out for RE–RE electrical coupling was two cells. GABA_A synapses were set at distances from three to five cells randomly, with probability 0.2. Each RE cell was modeled by a single compartment that included fast Na⁺ current, fast K⁺ current, low-threshold Ca²⁺-dependent current and K⁺ leak current described by Hodgkin–Huxley kinetics. GABA_A synaptic currents were modeled by first-order activation schemes (Destexhe *et al.*, 1996). Electrical coupling was modeled as $I_{ele} = g_{ele} (V_{pre} - V_{post})$, where g_{ele} is maximal conductance, $V_{pre} - V_{post}$ is pre – postsynaptic membrane potential. The voltage- and Ca²⁺-dependent transition rates for all intrinsic currents and the rate constants for all synaptic kinetic equations are given elsewhere (Bazhenov *et al.*, 1998).

Results

Characteristics of spikelets during spontaneous activity of RE neurons

Intracellular recordings from the rostral pole and rostromedial sector of the cat RE nucleus ($n = 49$) showed the characteristic

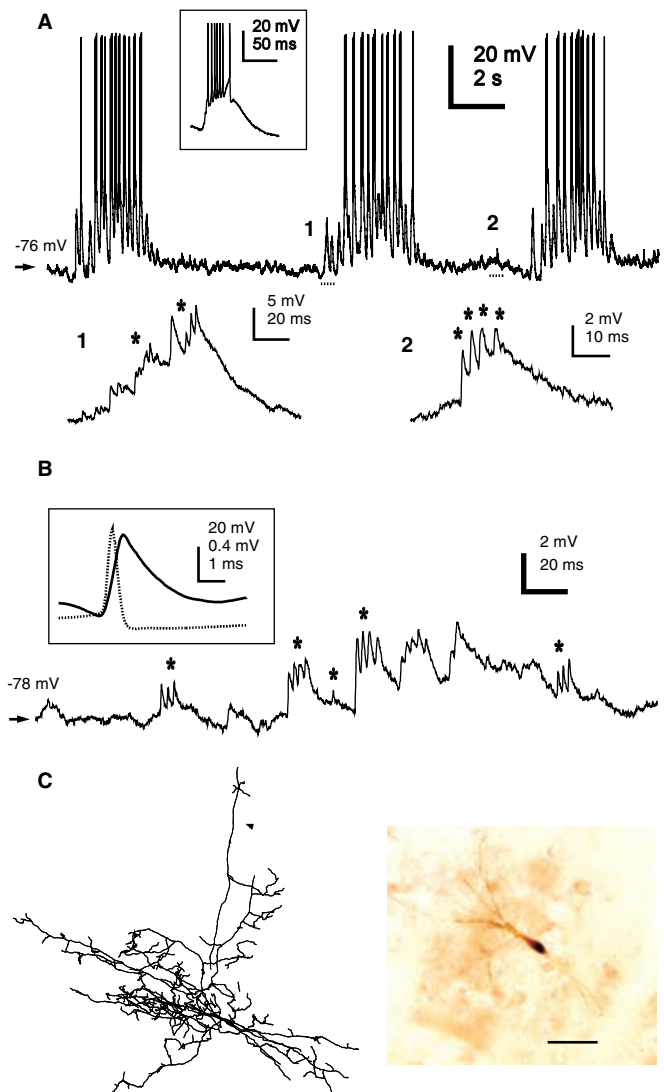


FIG. 1. Spikelets during spontaneous activity of RE neurons. Barbiturate anesthesia. (A) Spike-bursts over the depolarizing envelope of spindles. Typical low-threshold spike-burst of RE cell expanded in inset. Epochs marked 1 (at the onset of a spindle sequence) and 2 (during interspindle lull) are expanded below and show spikelets (asterisks), i.e. fast-rising and low-amplitude events occurring singly or in clusters. (B) Another RE neuron displaying spikelets (asterisks) occurring in isolation or in clusters. Inset shows the average ($n = 500$) of spikelets (solid line; scale bar: 0.4 mV), scaled with the average ($n = 500$) of full action potentials (dotted line; scale bar: 20 mV). (C) Intracellularly stained (neurobiotin) RE neuron located in the rostromedial sector of the nucleus. Photograph (right) and reconstruction (left). Arrowhead indicates the axon to the dorsal thalamus. Scale bar within the photograph: 0.1 mm for RE neuron in the photograph and 0.15 mm for the reconstructed neuron.

accelerando–decelerando pattern of their long spike-bursts that occurred over the depolarizing envelope of spindle sequences (inset in Fig. 1A), which are different from the shorter spike-bursts of thalamocortical neurons with progressively longer interspike intervals (Domich *et al.*, 1986; Contreras *et al.*, 1993). Invariably, small-amplitude, short-duration events were observed during spontaneous activity of all recorded RE neurons, regardless of the anesthesia (barbiturate, $n = 29$; urethane, $n = 10$; ketamine-xylazine, $n = 10$).

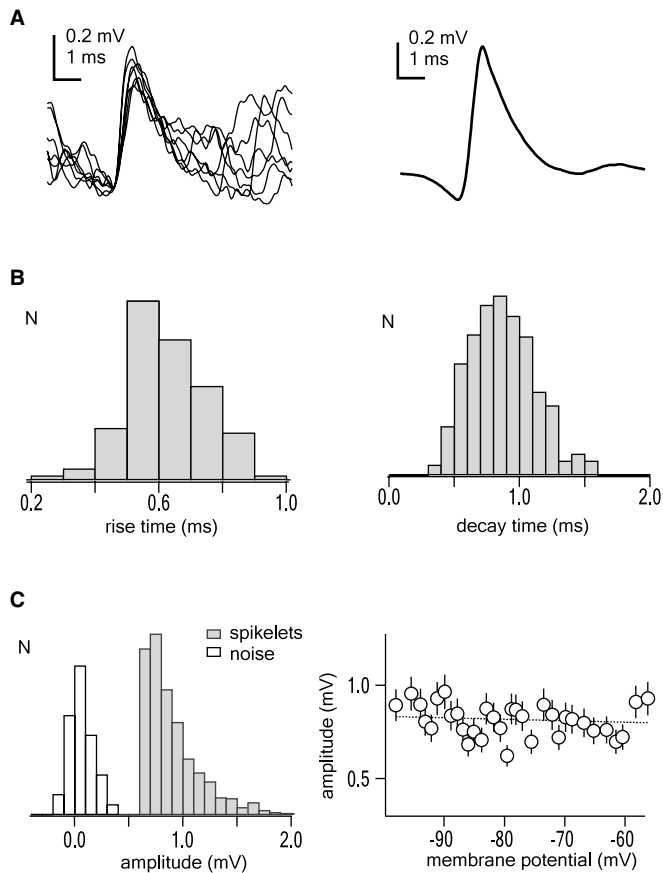


FIG. 2. Rise and decay phases, amplitudes and voltage-independency of spikelets. Barbiturate anesthesia. All panels from the same neuron. (A) Left, superimposition of spikelets in single traces; right, average ($n = 500$) of spikelets from a single RE neuron. (B) Left and right, histograms of rise time (10–90%) and decay phase (90–10%), respectively, for all spikelets in one neuron. (C) Left histogram shows amplitude distribution of spikelets. Right plot depicts the voltage-independency of spikelets' amplitudes (each point is the average of 10 individual points taken at the same membrane potential; dotted line is the best linear fitting for the group of points).

During barbiturate-induced spindling activity, RE neurons displayed prolonged spike-bursts over a depolarizing envelope and spikelets occurred during both spindle sequences and interspindle lulls (Fig. 1A and B). In addition to electrophysiological features that define RE neurons, some neurons located in the rostromedial sector of the nucleus adjacent to the ventrolateral nucleus were intracellularly stained and showed the typical aspect of RE neurons, with fusiform shape lying parallel to the surface of the dorsal thalamus and very long dendrites (Fig. 1C).

Generally, spikelets were much smaller (1.03 ± 0.04 mV, range 0.8–1.2 mV; $n = 25$) than action potentials, with a common amplitude ratio of $\approx 1 : 50$ (inset in Fig. 1B). In some neurons, however, spikelets reached amplitudes up to 3–5 mV (see Figs 3A and 5A). Spikelets were fast-rising (0.52 ± 0.1 ms, range 0.3–0.7 ms; $n = 25$) and fast-decaying (1.8 ms \pm 0.3 ms, range 0.8–3 ms; $n = 25$ neurons). The distributions of rise and decay times are shown for a representative RE neuron in Fig. 2B. Spikelets were voltage-independent for a large range of membrane potentials (Fig. 2C), thus suggesting their ubiquitous presence under physiological conditions.

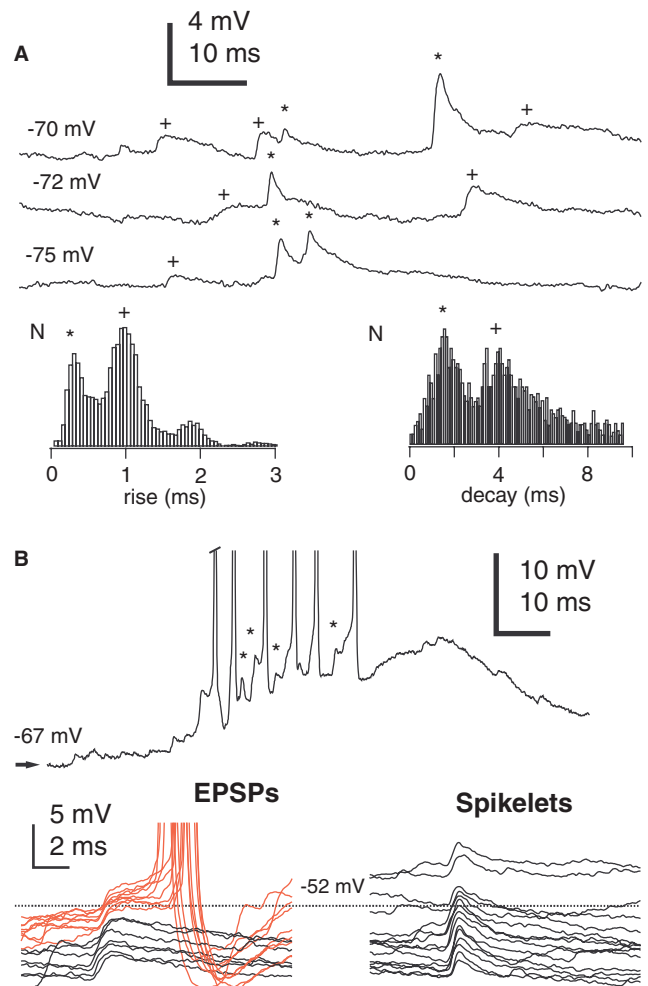


FIG. 3. Spikelets and EPSPs are different types of depolarizing events. (A) Barbiturate anesthesia. Top three traces, from the same RE neuron, show two types of depolarizations: spikelets (*) and EPSPs (+). Below, two histograms show the distribution of the rising and decaying phases (left and right, respectively) in the two types of events. (B) Ketamine-xylazine anesthesia, another neuron. Spikelets (*) are present during the firing of RE cell (spikes truncated). Note different rising phases in spikelets and some EPSPs that give rise to action potentials. Below, superimposed traces from the same neuron showing EPSPs and spikelets (see also text).

Spikelets are different from EPSPs and FPPs

To differentiate spikelets from depolarizing events triggered by synaptic mechanisms, such as EPSPs and FPPs, we first set the threshold for their detection at 0.6 mV, well beyond the maximum value of electronic noise that reached ≈ 0.3 –0.4 mV (see Fig. 2C). When all subthreshold events were considered (action potentials were excluded), the histograms of their amplitudes showed a continuously decreasing distribution from 0.6 to 5 mV (not shown). The duration of depolarizing events was selected at an empirical cutoff of 10 ms to encompass not only spikelets and FPPs but also slower depolarizations, such as EPSPs (see bottom left panel in Fig. 3B). As spikelets and EPSPs did not show differences in ranges of their amplitudes (0.5–6 mV), the rising and decaying phases were tested in all depolarizing events.

That spikelets and EPSPs were different events resulted from two major features. Firstly, we considered spikelets those events whose rising phase peaked at ≈ 0.5 ms and the decaying phase at ≈ 2 ms, whereas the same phases peaked at ≈ 1 ms and ≈ 4 ms in EPSPs (Fig. 3A). Thus, spikelets have much faster rising and decaying phases than EPSPs. Secondly, spikelets were unable to elicit full action potentials, even during states of membrane depolarization close to firing threshold, whereas EPSPs led to cell firing at the same level of depolarization (Fig. 3B). Modeling studies have suggested that the membrane time constant, τ_m , influences the delay between the onset of a given synaptic input and spike generation (Koch *et al.*, 1996), i.e. the generation of a full action potential is not instantaneous once the threshold is reached. It is then possible that fast events displaying very short durations, such as spikelets,

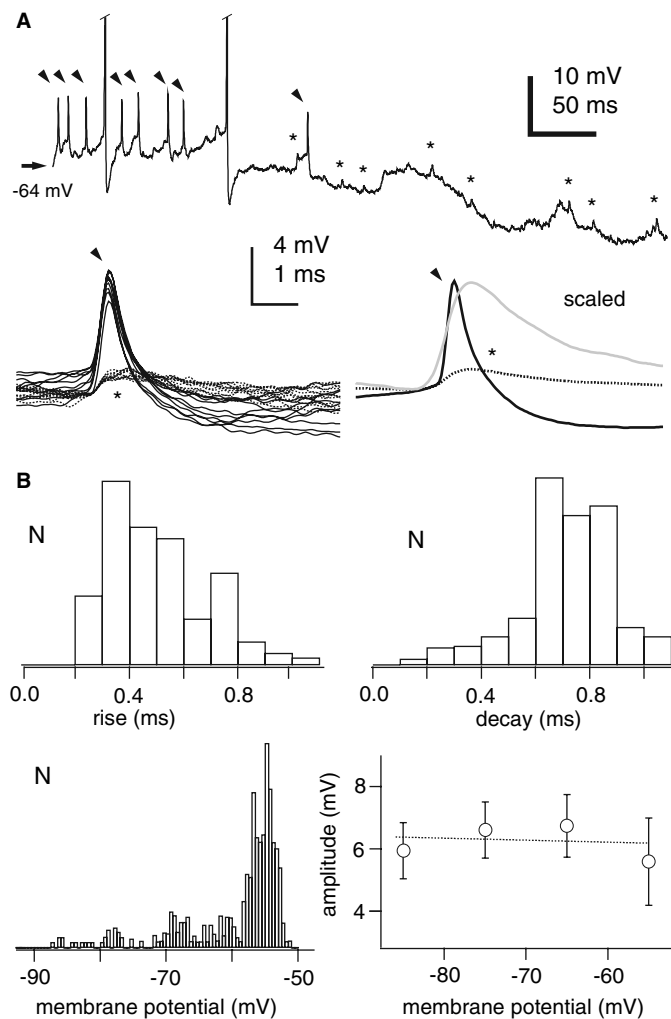


FIG. 4. Spikelets are also different from FPPs. Ketamine-xylazine anesthesia. (A) Top trace displays FPPs (arrowheads) and spikelets (*). Action potentials truncated. Below, superimposition of single events (left) and averages ($n = 100$) showing both FPPs and spikelets (right); the grey trace shows the averaged spikelet scaled ($\times 5$) for comparison. (B) Upper histograms show the rising and decaying phases (left and right, respectively) of FPPs. Bottom left histogram shows the voltage sensitivity of FPPs (compare with bottom right plot in Fig. 2 showing the voltage-independence of spikelets). Bottom right histogram shows voltage independence of the amplitude of FPPs. Each point is the average of 10 points taken from intervals of 10 mV.

do not generate full action potentials even if they reach the threshold for spike generation.

Spikelets could also be distinguished from FPPs, which are usually considered as dendritic spikes triggered by synaptic volleys. From the initial identification in hippocampal neurons (Spencer & Kandel, 1961), FPPs are characterized by rapid falling phase and initiation at ≈ 5 – 6 mV below the usual firing level. These synaptic events have been described in RE neurons where they were efficiently triggered by corticothalamic volleys (Contreras *et al.*, 1993) and in thalamocortical neurons (Maekawa & Purpura, 1967; Deschênes *et al.*, 1984; Steriade *et al.*, 1991; Timofeev & Steriade, 1997). In the present experiments, the amplitudes of FPPs were much greater than those of spikelets, and their time-course was also different (see scaled spikelet and FPP in Fig. 4A). In contrast to spikelets, FPPs were mainly present during periods of membrane depolarization; thus, comparison of the bottom right plot in Fig. 2C (spikelets) with bottom left histogram in Fig. 4B (FPPs) shows that FPPs are virtually absent at membrane potentials more negative than -70 mV. However, similarly to spikelets, the amplitudes of FPPs were not voltage-dependent (bottom right plot in Fig. 4B).

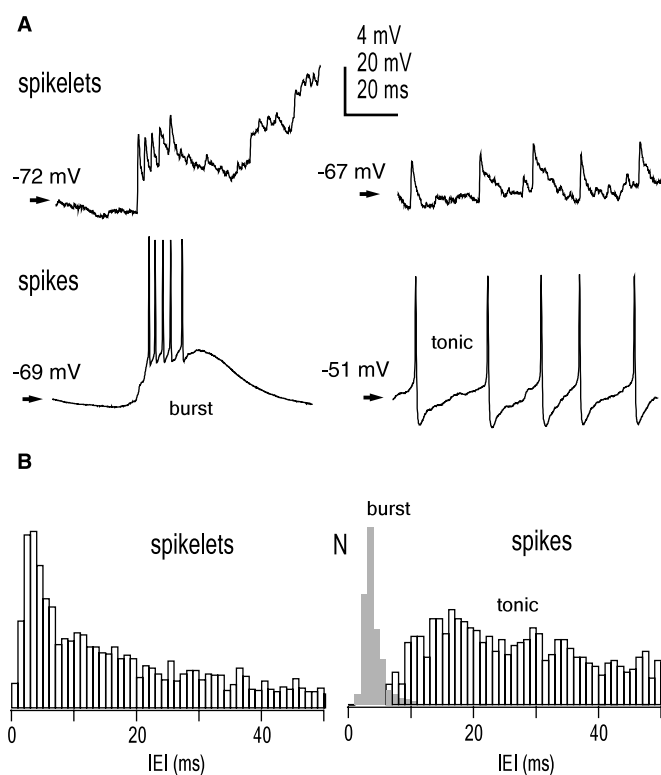


FIG. 5. Similarity between firing pattern of RE neurons and spikelets. Barbiturate anesthesia. (A) Traces displaying spikelets (top) and full action potentials (bottom). Left, clusters of spikelets separated by 2.5 ms and, below, spike-burst (≈ 350 Hz) from another RE neuron (same as the stained cell depicted in Fig. 1C). Right, individual spikelets and, below, tonic firing with the same frequency (≈ 50 Hz). Same two RE neurons as in the left panel. (B) Histograms with IEIs for spikelets and full action potentials from the two RE neurons, showing mode peaking at 3–4 ms for spike-bursts (grey colour in right histogram) and tonic firing in RE neuron firing action potentials, and similar distribution of IEIs in the other RE neuron firing spikelets. IEI, interevent interval.

Similarity between spikelets and firing patterns of RE neurons

RE neurons display two different modes of firing patterns: bursting, with intraburst frequencies up to 300–400 Hz, defining states associated with membrane hyperpolarization, as in natural slow-wave sleep (Steriade *et al.*, 1986) and anesthesia (Contreras *et al.*, 1993) or some types of seizures (Steriade & Contreras, 1995; Timofeev *et al.*, 1998); and tonic, with single spikes at frequencies between 40 and 80 Hz, characteristic for the waking state (Steriade *et al.*, 1986). Figure 5 shows two RE neurons recorded in different experiments, one of them displaying spikelets, the other full action potentials. The frequency of clusters formed by spikelets (≈ 350 –400 Hz) and that of individual spikelets (≈ 40 –50 Hz) in one RE neuron were similar to frequencies of spike-bursts and tonic firing displayed by the other RE neuron. Histograms of interevent intervals also demonstrate the two firing modes in both neurons, with an early peak at 3–4 ms, reflecting frequencies of spike-bursts and clusters of spikelets (which both predominated during recordings), and widely distributed intervals during the tonic mode, mainly between 10 and 20 ms.

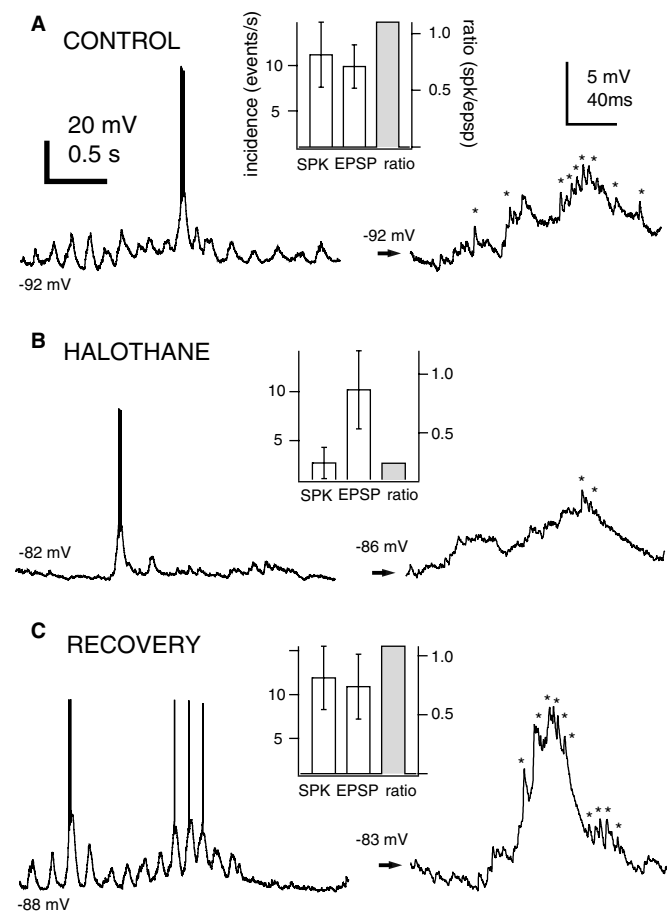


Fig. 6. Spikelets are strongly reduced or virtually abolished by halothane. Barbiturate anesthesia. Left column, different epochs before (A), during halothane administration (B), and recovery of initial state after halothane (C). Right column, expanded periods from neurons depicted in the left column. Insets: incidence of spikelets (SPK) and EPSPs (left ordinate), and their ratio during a 5-min period of recording (right ordinate) in each of the three states.

Origin of spikelets

To determine the origin of spikelets, several manipulations were performed. Decortication or addition of QX-314 or KCl in the recording pipette had no effect on the amplitudes or incidence of spikelets (not shown). By contrast, administration of halothane (5%, 2–5 min; $n = 4$), a gap junction blocker, invariably decreased the incidence of spikelets, without changing their amplitudes and durations (Fig. 6). Halothane blocked the occurrence of spindle sequences under barbiturate anesthesia. Its action lasted for 7–8 min, with complete recovery after 10 min. The strongest observed effect was on spikelets. The ratio between spikelets and EPSPs, recorded during periods of 5 min in all three states (before, during and after halothane administration) showed a fivefold decrease from control to halothane, with subsequent recovery to the control value.

Role of gap junctions in synchronization of spindling activity in the thalamus

In order to test a possible role of gap junctions in the synchronization of activity in the RE nucleus, simultaneous dual, triple and quadruple extracellular recordings of RE neurons were performed in decorticated cats under barbiturate anesthesia, and auto- and cross-correlation analyses were carried out before and after the application of halothane (4%, 2–3 min). Decortication was performed to avoid any corticothalamic influences. During the control period (5–10 min), neurons displayed oscillatory activity in the spindle frequency (≈ 10 Hz) (Fig. 7A). Such activity was highly correlated between the different pairs of cells (Fig. 7A). Upon the application of halothane (4%, 2–3 min), RE neurons changed their behavior. Instead of the rhythmic firing characteristic of spindle activity, each neuron displayed burst and tonic firing in an apparently random way (Fig. 7B). Such activity did not represent spindle waves, as 10 Hz activity disappeared from both auto- and cross-correlograms (Fig. 7B). Thus, halothane did not seemingly affect the firing rates of RE neurons, but their rhythmicity, in particular that in the frequency range of spindles. Note that some neuronal couples (1–3, 2–4, 1–4) maintained high correlation in the presence of halothane, but only for high frequencies, whereas correlations in the frequency range of spindles was invariably impaired (Fig. 7B). When halothane administration was stopped, spindling activity recovered slowly in all neurons until the control pattern was completely restored (Fig. 7C). Not only the spindling frequency recovered, but also the phase lags between the different neuronal pairs were similar to those in the control (Fig. 7C). These results suggest a role for electrical coupling in the synchronization of spindle activity in the RE nucleus.

Modeling experiments predict a role for gap junctions in spreading of slow activities in the thalamus

To test a possible effect of gap junction between RE cells, a pair of electrically connected neurons was modeled. When both cells were held at relatively depolarized potentials, a single spike in the presynaptic cell induced a spikelet in the postsynaptic cell, with amplitude matching experimental data (Fig. 8A, top trace and inset). Hyperpolarization of the presynaptic RE cell de-inactivated T-channels, so the same stimulus induced a low-threshold spike (LTS) followed by a burst of fast action potentials (Fig. 8A, second trace). This relatively slow process was transmitted better through the

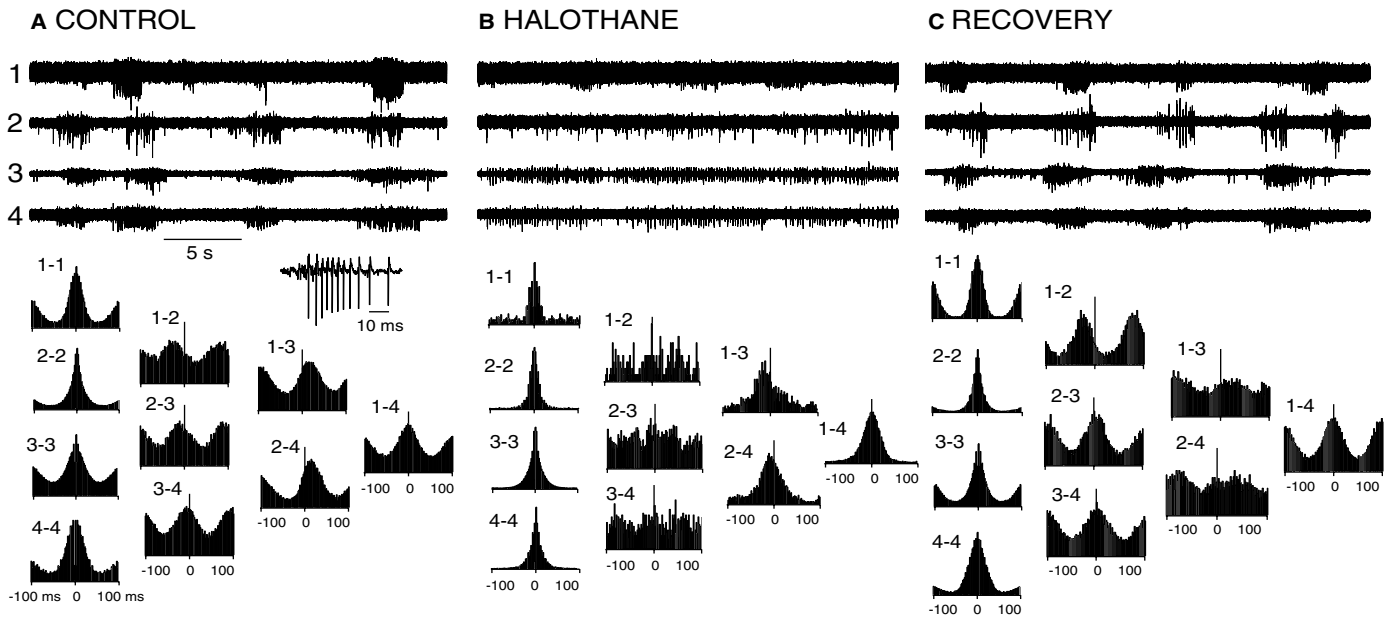


FIG. 7. The role of gap junctions in spindle synchronization. Simultaneous quadruple extracellular recordings of RE neurons were performed in decorticated cats under barbiturate anesthesia. Neighbor electrodes were separated by ≈ 0.5 mm (1 represents the most anteriorly located neuron and 4 the most posterior). RE neurons were identified in each case by their long bursts (> 50 ms) and the accelerando–decelerando firing pattern (see inset in A, burst extracted from cell 2). (A) CONTROL shows 30 s of normal activity of four RE neurons during barbiturate anesthesia, with recurrent spindles each 2–5 s. At the bottom, auto- and cross-correlograms are depicted for 5 min of recording. Note highly correlated ≈ 10 Hz activity in all cases. (B) HALOTHANE illustrates the effect of halothane (4%, 2 min) on RE neurons. Note the loss of correlation between pairs of cells and the absence of activity at 10 Hz. (C) RECOVERY, when halothane administration stopped, RE neurons recovered the pattern of activity displayed in the control period.

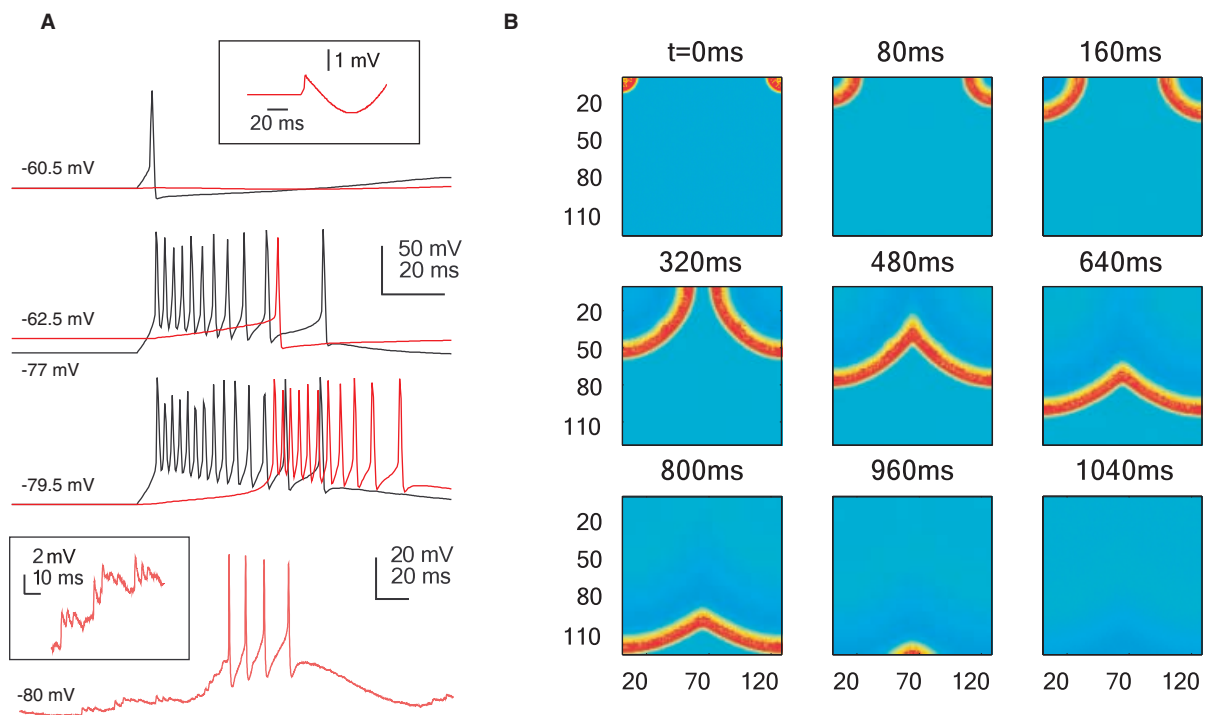


FIG. 8. Role of gap junctions between RE cells in initiating LTS and wave propagation. (A) Model of a pair of reciprocally connected RE cells. Spikelet (see inset) was induced in the postsynaptic cell (red line) by single spike in the presynaptic neuron (black line). Upon hyperpolarization of presynaptic neuron (second trace), a burst of spikes can trigger a single spike in the postsynaptic neuron. When both cells are hyperpolarized (third trace), a burst in the presynaptic cell can induce a delayed spike-burst in the postsynaptic cell. Bottom trace represents intracellular recording of RE neuron *in vivo* (see text). (B) Wave dynamics in two-dimensional network of RE neurons. Two stimuli were applied simultaneously at the corners of a two-dimensional 128×128 network of RE cells interconnected with gap junctions. Firing cells are shown in red, silent neurons indicated by blue.

electrical synapse and the progressive depolarization of the postsynaptic cell during the spike-burst led to a Na^+ spike (Fig. 8A, second trace). Finally, when both neurons were hyperpolarized (Fig. 8A, third trace), the electrical coupling-dependent depolarization of the postsynaptic RE neuron triggered an LTS, suggesting that gap junctions may spread activity between connected cells. Intracellular recordings *in vivo* (Fig. 8A, bottom trace) indeed showed that it was rather common to see after a sequence of spikelets' clusters, the RE neuron to reach the state at which a spike-burst was generated (see inset in Fig. 8A). We should note that although the amplitude of simulated spikelets was similar to that in experimental data, the time course was different, i.e. the action potentials in the model were wider than in experimental data (Fig. 8A) because of the properties of simulated action potentials that generated spikelets. Also, simulated spikelets displayed a prominent hyperpolarizing component after the decaying phase, generated by low-pass filtering of action potentials' afterhyperpolarizing potential, a component that was rarely seen in the present intracellular recordings.

To study the network effect of electrical coupling, a one-dimensional chain of RE neurons was simulated. Gap junctions were introduced between RE neurons within a two-neuron footprint. GABA_A synapses were included between RE neurons more than two cells apart and within a five-cell radius with a sparse GABA_A-mediated connectivity with probability 0.2. When an external stimulus was applied to the cells at the end of the chain, a wave of activation propagated with constant velocity (not shown). In a two-dimensional network of RE cells (128×128) interconnected via gap junctions, the same mechanism mediated either plane waves (Fig. 8B) or self-sustained spiral waves (not shown). Electrical coupling mediated rebound LTS and wave propagation. Inactivation of Ca^{2+} -dependent LTS after burst discharges precipitated the refractory period, so the waves disappeared after collapsing in the middle of the network.

These results suggest that gap junctions can mediate spread of activity not only between electrically connected neurons but also at great distances.

Discussion

Our results show that RE neurons investigated *in vivo* display small but rapidly rising and decaying potentials, termed spikelets in recent *in vitro* studies on RE (Landisman *et al.*, 2002) and thalamocortical (Hughes *et al.*, 2002) neurons, which are a sign of electrotonic coupling. In the absence of definitive dual intracellular recordings from neighboring RE neurons, the evidence indicates that spikelets recorded in our experiments were not synaptically triggered events: (1) spikelets displayed much faster rising and decaying phases than EPSPs (Fig. 3A) and their amplitudes were much lower than those of FPPs (Fig. 4); (2) spikelets did not trigger action potentials, as already reported in electrotonically coupled inferior olivary neurons (Devor & Yarom, 2002), in contrast to the ability of EPSPs to promote spiking at the same level of membrane potential (Fig. 3B); (3) their frequency in both cluster and single-event modes was virtually identical to those of full action potentials in other RE neurons during these two firing modes (Fig. 5); and (4) spikelets were blocked by halothane (Fig. 6), a gap junction blocker (Draguhn *et al.*, 1998; Moortgat *et al.*, 2000). Additionally, spikelets are not dependent on synaptic inputs from cortex, as is the case of FPPs that are most efficiently triggered by cortico-RE volleys (Contreras *et al.*, 1993), as they occurred without changes in incidence and

shape/amplitude in decorticated animals. Also, recordings with KCl-filled micropipettes, to reverse GABA_A-receptor-mediated potentials, did not affect their characteristic features.

The time-course and amplitudes of spikelets documented here are very similar to those described in slices from RE nucleus (Landisman *et al.*, 2002). Some differences between the characteristics of presently described spikelets in RE neurons and spikelets recorded *in vitro* from thalamic dLG neurons (Hughes *et al.*, 2002) are as follows: (1) in dLG neurons spikelets were present in a subset of cells (17–19%), whereas all 49 of the presently recorded RE neurons displayed such events; (2) the amplitudes of dLG spikelets were more than twice as high (range 2–7 mV) as in the presently recorded RE neurons (range 0.8–1.2 mV); and (3) with few exceptions the waveform of dLG spikelets was similar to that of conventional PSPs, whereas RE-cells' spikelets displayed significantly faster rising and decaying times than EPSPs. These differences might be ascribed to the large family of connexins, with particular distributions and characteristics (Goodenough *et al.*, 1996).

Although electrotonic coupling has been described in a variety of central structures in mammals, among them neocortex (Galarreta & Hestrin, 1999; Gibson *et al.*, 1999), hippocampus (Draguhn *et al.*, 1998), thalamus (Hughes *et al.*, 2002; Landisman *et al.*, 2002) and inferior olive (Llinás *et al.*, 1974; Lampl & Yarom, 1997; Devor & Yarom, 2002), at least for neocortex it is common in early stages of circuit formation and decreases during later development (Connors *et al.*, 1983; Peinado *et al.*, 1993). Among the exceptions to this rule are the inferior olive in which the morphological correlate of the electrotonic coupling, gap junctions, is present at birth (Bourat & Sotelo, 1983), and RE neurons in which spikelets were recorded in the present experiments on adult cats. In these two structures, the role of electrotonic coupling may be that of a synchronizing device.

Experimental and modeling studies have shown that electrotonic coupling underlies the rhythmicity of complex spike activity in the olivo-cerebellar pathway (Welsh & Llinás, 1997; Makarenko & Llinás, 1998; Loewenstein *et al.*, 2001). A combination of electrical and chemical synapses among local-circuit basket inhibitory neurons has been proposed to entrain fast rhythms, in the gamma frequency range, in rat neocortex (Tamás *et al.*, 2000), and electrical synapses are also thought to generate gamma oscillations in the hippocampus (Draguhn *et al.*, 1998; Traub *et al.*, 1999a,b).

As to the RE nucleus, besides chemical synapses among these GABAergic neurons, which have been implicated in the generation and synchronization of spindle rhythms in experimental (Steriade *et al.*, 1987) and modeling (Destexhe *et al.*, 1994; Golomb *et al.*, 1994; Bazhenov *et al.*, 1999) studies, electrotonic coupling may be an additional, if not the leading, factor in this synchronizing process. In fact, the simulations presented here show that activity in the RE nucleus can spread not only between pairs of neighboring electrotonically coupled neurons (Fig. 8A) but also at greater distances (Fig. 8B). This spreading activity could not be due to single spikelets because they are not able to trigger action potentials (Fig. 3B). However, LTSs may be able to activate a neighbor cell and thus contribute to the propagation and synchronization of spindle activity (Fig. 7). This could be expected due to the low-pass properties of gap junctions (Landisman *et al.*, 2002), which strongly filter fast signals (such as action potentials) but not slower signals (such as LTSs). In our experiments the incidence of spikelets decreased during halothane application. As to a possible reduction in spikelets' amplitudes, this cannot be discarded but, under normal recording conditions, spikelets already displayed small

amplitudes, sometimes close to the level of noise. In the study on electrotonic coupling between RE neurons maintained *in vitro* (Landisman *et al.*, 2002), it was also concluded that, although spike-to-spike synchronization was precluded in all but the most strongly coupled cell groups, electrical synapses may be effective in some normal and paroxysmal rhythmical activities. Besides a role in spreading slow activities in the RE nucleus, predicted by modeling studies (Fig. 8), we hypothesized (Fuentealba *et al.*, 2002) and the present experimental data (Fig. 7) support the idea that electrical coupling may be important for the synchronization of spindle activities.

Acknowledgements

This work was supported by grants from the Canadian Institutes for Health Research (MT-3689, MOP-36545 and MOP-37862), US National Institutes of Health (NS-40522), Fonds de recherche en santé du Québec and The Howard Hughes Medical Institute. We thank P. Giguère and D. Drolet for technical assistance.

Abbreviations

dLG, dorsal part of the lateral geniculate nucleus; EPSP, excitatory postsynaptic potential; FPP, fast prepotential; GABA, γ -aminobutyric acid; LTS, low-threshold spike; RE, thalamic reticular nucleus.

References

- Avanzini, G., De Curtis, M., Pape, H.C. & Spreafico, R. (1999) Intrinsic properties of reticular thalamic neurons relevant to genetically determined spike-wave generation. In: Delgado-Escueta, A.V., Wilson, W.A., Olsen, R.W. & Porter, R.J. (Eds), *Jasper's Basic Mechanisms of the Epilepsies*. Lippincott, Williams & Wilkins, Philadelphia, p. 297–309.
- Bazhenov, M., Timofeev, I., Steriade, M. & Sejnowski, T.J. (1998) Cellular and network models for intrathalamic augmenting responses during 10-Hz stimulation. *J. Neurophysiol.*, **79**, 2730–2748.
- Bazhenov, M., Timofeev, I., Steriade, M. & Sejnowski, T.J. (1999) Self-sustained rhythmic activity in the thalamic reticular nucleus mediated by depolarizing GABAA receptor potentials. *Nature Neurosci.*, **2**, 168–174.
- Bourat, F. & Sotelo, C. (1983) Postnatal development of the inferior olivary complex in the rat. I. An electronic microscopic study of the medial accessory olive. *Dev. Brain Res.*, **8**, 291–310.
- Condorelli, D.F., Belluard, N., Trovato-Salinaro, A. & Mudo, I. (2000) Expression of Cx36 in mammalian neurons. *Brain Res. Rev.*, **32**, 72–85.
- Connors, B.W., Bernardo, L.S. & Prince, D.A. (1983) Coupling between neurons of the developing rat neocortex. *J. Neurosci.*, **3**, 773–782.
- Contreras, D., Curró Dossi, R. & Steriade, M. (1993) Electrophysiological properties of cat reticular neurones *in vivo*. *J. Physiol. (Lond.)*, **470**, 273–294.
- Deschênes, M., Paradis, M., Roy, J.P. & Steriade, M. (1984) Electrophysiology of neurons of lateral thalamic nuclei in cat: resting properties and burst discharges. *J. Neurophysiol.*, **51**, 1196–1219.
- Destexhe, A., Bal, T., McCormick, D.A. & Sejnowski, T.J. (1996) Ionic mechanisms underlying synchronized and propagating waves in a model of ferret thalamic slices. *J. Neurophysiol.*, **76**, 2049–2070.
- Destexhe, A., Contreras, D., Sejnowski, T.J. & Steriade, M. (1994) A model of spindle rhythmicity in the isolated thalamic reticular nucleus. *J. Neurophysiol.*, **72**, 803–818.
- Devor, A. & Yarom, Y. (2002) Electrotonic coupling in the inferior olivary nucleus revealed by simultaneous double patch recordings. *J. Neurophysiol.*, **87**, 3048–3058.
- Domich, L., Oakson, G. & Steriade, M. (1986) Thalamic burst patterns in the naturally sleeping cat: a comparison between cortically projecting and reticularis thalami neurons. *J. Physiol. (Lond.)*, **379**, 429–449.
- Draguhn, A., Traub, R.D., Schmitz, D. & Jefferys, J.G. (1998) Electrical coupling underlies high-frequency oscillations in the hippocampus *in vitro*. *Nature*, **394**, 189–192.
- Fuentealba, P., Crochet, S., Timofeev, I. & Steriade, M. (2002) 'Spikelets' in cat thalamic reticular nucleus *in vivo*. *Soc. Neurosci. Abstr.*, **28**, 144. 19.
- Galarreta, M. & Hestrin, S. (1999) A network of fast-spiking cells in the neocortex connected by electrical synapses. *Nature*, **402**, 72–75.
- Gibson, J.R., Beierlein, M. & Connors, B.W. (1999) Two networks of electrically coupled inhibitory neurons in neocortex. *Nature*, **402**, 75–79.
- Golomb, D., Wang, X.J. & Rinzel, J. (1994) Synchronization properties of spindle oscillations in a thalamic reticular nucleus model. *J. Neurophysiol.*, **72**, 1109–1126.
- Goodenough, D.A., Goliger, J.A. & Paul, D.L. (1996) Connexins, connexons, and intercellular communications. *Ann. Rev. Biochem.*, **65**, 475–502.
- Hughes, S.W., Blethyn, K.L., Cope, D.W. & Crunelli, V. (2002) Properties and origin of spikelets in thalamocortical neurones *in vitro*. *Neuroscience*, **110**, 395–401.
- Koch, C., Rapp, M. & Segev, I. (1996) A brief history of time (constants). *Cereb. Cortex*, **6**, 93–101.
- Lampl, I. & Yarom, Y. (1997) Subthreshold oscillations and resonant behavior: two manifestations of the same mechanism. *Neuroscience*, **78**, 325–341.
- Landisman, C.E., Long, M.A., Beierlein, M., Deans, M.R., Paul, D.L. & Connors, B.W. (2002) Electrical synapses in the thalamic reticular nucleus. *J. Neurosci.*, **22**, 1002–1009.
- Llinás, R., Baker, R. & Sotelo, C. (1974) Electrotonic coupling between neurons in cat inferior olive. *J. Neurophysiol.*, **37**, 560–571.
- Loewenstein, Y., Yarom, Y. & Sompolinsky, H. (2001) The generation of oscillations in networks of electrically coupled cells. *Proc. Natl Acad. Sci. USA*, **98**, 8095–8100.
- Maekawa, K. & Purpura, D.P. (1967) Properties of spontaneous and evoked activities of thalamic ventrobasal neurons. *J. Neurophysiol.*, **30**, 360–381.
- Makarenko, V. & Llinás, R. (1998) Experimentally determined chaotic phase synchronization in a neuronal system. *Proc. Natl Acad. Sci. USA*, **95**, 15747–15752.
- Moortgat, K.T., Bullock, T.H. & Sejnowski, T.J. (2000) Precision of the pacemaker nucleus in a weakly electric fish: network vs. cellular influences. *J. Neurophysiol.*, **83**, 971–983.
- Peinado, A., Yuste, R. & Katz, L.C. (1993) Extensive dye coupling between rat neocortical neurons during the period of circuit formation. *Neuron*, **10**, 103–114.
- Perez-Velazquez, J.L. & Carlen, P.L. (2000) Gap junctions, synchrony and seizures. *Trends Neurosci.*, **23**, 68–74.
- Rash, J.E., Staines, W.A., Yasumura, T., Patel, D., Furman, C.S., Stelmack, G.L. & Nagy, J.I. (2000) Immunogold evidence that neuronal gap junctions in adult rat brain and spinal cord contain connexin-36 but not connexin-32 or connexin-43. *Proc. Natl Acad. Sci. USA*, **97**, 7573–7578.
- Spencer, W.A. & Kandel, E.R. (1961) Electrophysiology of hippocampal neurons. IV. Fast prepotentials. *J. Neurophysiol.*, **24**, 272–285.
- Steriade, M. & Contreras, D. (1995) Relations between cortical and thalamic cellular events during transition from sleep pattern to paroxysmal activity. *J. Neurosci.*, **15**, 623–642.
- Steriade, M., Curró Dossi, R., Paré, D. & Oakson, G. (1991) Fast oscillations (20–40 Hz) in thalamocortical systems and their potentiation by mesopontine cholinergic nuclei in the cat. *Proc. Natl Acad. Sci. USA*, **88**, 4396–4400.
- Steriade, M., Deschênes, M., Domich, L. & Mulle, C. (1985) Abolition of spindle oscillations in thalamic neurons disconnected from nucleus reticularis thalami. *J. Neurophysiol.*, **54**, 1473–1497.
- Steriade, M., Domich, L. & Oakson, G. (1986) Reticularis thalami neurons revisited: activity changes during shifts in states of vigilance. *J. Neurosci.*, **6**, 68–81.
- Steriade, M., Domich, L., Oakson, G. & Deschênes, M. (1987) The deafferented reticularis thalami nucleus generates spindle rhythmicity. *J. Neurophysiol.*, **57**, 260–273.
- Steriade, M., McCormick, D.A. & Sejnowski, T.J. (1993) Thalamocortical oscillation in the sleeping and aroused brain. *Science*, **262**, 679–685.
- Tamás, G., Buhl, E.H., Lorincz, A. & Somogyi, P. (2000) Proximally targeted GABAergic synapses and gap junctions synchronize cortical interneurons. *Nature Neurosci.*, **3**, 366–371.
- Timofeev, I., Grenier, F. & Steriade, M. (1998) Spike-wave complexes and fast runs of cortically generated seizures. IV. Paroxysmal fast runs in cortical and thalamic neurons. *J. Neurophysiol.*, **80**, 1495–1513.
- Timofeev, I. & Steriade, M. (1997) Fast (mainly 30–100 Hz) oscillations in the cat cerebellothalamic pathway and their synchronization with cortical potentials. *J. Physiol. (Lond.)*, **504**, 153–168.

- Traub, R.D., Jefferys, J.G.R. & Whittington, M.A. (1999b) *Fast Oscillations in Cortical Circuits*. MIT Press, Cambridge, MA.
- Traub, R.D., Schmitz, D., Jefferys, J.G.R. & Draguhn, A. (1999a) High-frequency population oscillations are predicted to occur in hippocampal pyramidal neuronal networks interconnected by axoaxonal gap junctions. *Neuroscience*, **92**, 407–426.
- Venance, L., Rozov, A., Blatow, M., Burnashev, N., Feldmeyer, D. & Monyer, H. (2000) Connexin expression in electrically coupled postnatal rat brain neurons. *Proc. Natl Acad. Sci. USA*, **97**, 10260–10265.
- Welsh, J.P. & Llinás, R. (1997) Some organizing principles for the control of movement based on olivocerebellar physiology. *Progr. Brain Res.*, **114**, 449–461.